INTERFACE

royalsocietypublishing.org/journal/rsif

Research

Cite this article: Rooker JR *et al*. 2026 Otolith geochemistry of tropical and temperate tunas in the ocean. *J. R. Soc. Interface* **23**: 20250814.
https://doi.org/10.1098/rsif.2025.0814

Received: 5 August 2025
Accepted: 5 January 2026

Subject Category:
Life Sciences–Chemistry interface

Subject Areas:
biogeochemistry, ecosystem, environmental science

Keywords:
population connectivity, highly migratory, metapopulation, otolith geochemistry, *Thunnus*, niche breadth, natal origin

Author for correspondence:
Jay R. Rooker
e-mail: rookerj@tamug.edu

Electronic supplementary material is available online at https://doi.org/10.6084/m9.figshare.c.8285018.

THE ROYAL SOCIETY PUBLISHING

Otolith geochemistry of tropical and temperate tunas in the ocean

Jay R. Rooker[1], R.J. David Wells[1], Iraide Artetxe-Arrate[2], Haritz Arrizabalaga[2], Igaratza Fraile[2], Michael A. Dance[3], Patricia Lastra Luque[2], Laia Munoz[4], Alexandra Prouse[1], Shane A. Stephens[1], Natalie Windels[1] and Michelle Zapp Sluis[1]

[1]Department of Marine Biology, Texas A&M University, Galveston, TX, USA
[2]AZTI, Marine Research, Basque Research and Technology Alliance (BRTA), Pasaia, Gipuzkoa, Spain
[3]Department of Oceanography and Coastal Sciences, Louisiana State University System, Baton Rouge, LA, USA
[4]Department of Oceans, Stanford University, Stanford, CA, USA

JRR, 0000-0002-5934-7688; R.JDW, 0000-0002-1306-0614

Geographic trends in otolith $\delta^{18}O$ and $\delta^{13}C$ provide insights into relevant spatial scale(s) of population discrimination, and the utility of these geochemical markers for elucidating the movements, stock structure and niche breadth in fishes. Otolith $\delta^{18}O$ and $\delta^{13}C$ of juvenile (age-0/1) tunas (genus *Thunnus*) were quantified to characterize regional and global variation across the Atlantic, Pacific and Indian Oceans. Tunas from the Atlantic Ocean commonly displayed higher otolith $\delta^{18}O$ relative to individuals from comparable zones (tropical or temperate) in the Pacific Ocean, and to a lesser degree, the Indian Ocean. Otolith $\delta^{18}O$ of tunas collected at higher latitudes was elevated and more variable, with temperate tunas (albacore, Atlantic and Pacific bluefin) enriched in otolith ^{18}O relative to congeners in tropical waters (bigeye, blackfin and yellowfin). Inter- and intra-ocean trends in otolith $\delta^{13}C$ were less pronounced, but tunas collected from several regions in the Atlantic Ocean were generally enriched in otolith ^{13}C relative to individuals from the Pacific and Indian Oceans. Niche breadth derived from otolith $\delta^{18}O$ and $\delta^{13}C$ was often wider for tunas collected in temperate zones where individuals experience more variable environmental conditions compared with congeners in tropical waters.

1. Background

Large pelagic fishes (billfishes, tunas and sharks) are top predators in marine ecosystems and play important ecological roles by influencing the structure and dynamics of open-ocean food webs through top-down control [1,2]. Many of these pelagic fishes are classified as highly migratory and commonly move long distances, often traversing multiple jurisdictional boundaries and/or large marine ecosystems throughout their life cycles [3,4]. Sustainable management of highly migratory species requires data on their natal origin, migration pathways and population structure as well as extrinsic drivers influencing spatial displacements. Our understanding of the migration ecology of top predators in the ocean has increased significantly in the past few decades through the application of satellite and acoustic telemetry [4,5], genomics [6,7] and geochemical tags [8,9], with the latter approach showing considerable promise for retrospective determination of natal origin and population mixing at the ocean-basin scale [10,11]. Given the demographic implications of spatio-temporal shifts in distributions in response to global climate change and other anthropogenic stressors, there is a clear need to improve our understanding of the population connectivity of pelagic fishes.

Over the past three decades, research using geochemical tags (trace elements and stable isotopes) in the otoliths (ear stones) has provided novel insights into the origin and migratory behaviours of true tunas (genus *Thunnus*) in the Atlantic Ocean [12–15], Pacific Ocean [16–18] and Indian Ocean [19,20]. In addition, geochemical life history profiles (i.e. chronologies) across the entire otolith (core to margin) have been used to elucidate age-specific patterns of egress/ingress between different ecosystems or regions (e.g. shifts from coastal nurseries to offshore foraging areas) [21,22]. Data on the spatial and temporal complexities of tunas derived from different applications of these natural tags has proven critical to the management of tunas by international conventions, including the International Commission for the Conservation of Atlantic Tunas (ICCAT), Indian Ocean Tuna Commission (IOTC) and Inter-American Tropical Tuna Commission (IATTC) [23]. Specifically, the integration of spatio-temporal distribution data on populations into operational models reduces bias in stock assessments and improves estimations of biological reference points required to sustainably manage populations of tunas and other species [24,25].

Stable oxygen ($\delta^{18}O$) and carbon ($\delta^{13}C$) isotopes in otoliths are reflective of physico-chemical conditions (e.g. temperature and salinity) of seawater and diet/metabolic processes, respectively. Both serve as natural geochemical markers [26] that afford information on the origin and migratory histories of tunas and other highly migratory species [8,27]. Here, we present data from a comprehensive meta-analysis for otolith $\delta^{18}O$ and $\delta^{13}C$ values of juvenile tunas collected at the global scale to characterize inter- and intra-ocean variation of individuals from tropical and temperate waters of the Atlantic, Pacific and Indian Oceans. Our analysis is based on incorporating otolith $\delta^{18}O$ and $\delta^{13}C$ values from cross-sectional studies on six species of true tunas (genus *Thunnus* spp.); three tropical species (bigeye [*T. obesus*], blackfin [*T. atlanticus*] and yellowfin [*T. albacares*]) and three temperate species (albacore [*T. alalunga*], Atlantic bluefin [*T. thynnus*] and Pacific bluefin [*T. orientalis*]). We first evaluate whether otolith $\delta^{18}O$ and $\delta^{13}C$ in juvenile congeners collected from the same region/year display comparable values to determine whether pooling *Thunnus* species is appropriate for large-scale regional characterizations. Next, we characterize regional variation in otolith $\delta^{18}O$ and $\delta^{13}C$ values and develop isoscapes incorporating data from all three oceans to describe the spatial resolution of both markers for discriminating individuals from different production zones. Finally, we quantify the geochemical niche breadth for regional populations of tunas based on otolith $\delta^{18}O$ and $\delta^{13}C$ values to shed light on niche dynamics and environmental conditions experienced by juveniles across the three ocean basins. Our basic premise for using this approach is that variability in environmental conditions experienced by juvenile tunas will influence niche breadth, and thus we hypothesize that variable or shifting biological (prey) and/or physico-chemical conditions experienced by tuna in a region will result in a wider niche breadth.

2. Methods

Juvenile (age-0/1) tunas used in this study (n = 1587) were collected from 1998 to 2022 from multiple tropical and temperate locations in the Atlantic Ocean, Pacific Ocean and Indian Ocean and associated marginal seas (e.g. Mediterranean Sea, Gulf of Mexico, Sea of Japan, East China Sea) (table 1). Since the aim of this study was to develop a geographic characterization of otolith $\delta^{18}O$ and $\delta^{13}C$ for tunas at the global scale, samples were restricted to juveniles to limit the potential for movements between major geographic zones prior to collection. Our assessment is based predominantly on otolith core material from age-0 tunas (79%; mean size: 37.1 cm fork length [FL]); however, age-1 individuals were included for albacore and Atlantic bluefin tuna (mean size: 61.5 cm FL) from areas adjacent or close to presumed nursery areas to expand the spatial coverage of available data for temperate tunas. Otolith $\delta^{18}O$ and $\delta^{13}C$ data for tunas includes original unpublished data and data derived from published studies (electronic supplementary material, table S1). Juvenile tunas were collected from recreational and commercial fisheries as well as from scientific sampling campaigns, and all collections were performed in accordance with relevant guidelines and regulations of institutional animal care and use committees.

Sagittal otoliths of juvenile tunas were extracted, cleansed of adhering tissue, rinsed with deionized water (DIH_2O) and stored dry in plastic vials. One otolith from each specimen was selected at random from the pair, embedded in EpoFix resin (Struers A/S) and sectioned with a low-speed saw to expose the otolith core, following established protocols [13] that were generally consistent across a wide range of studies. Thin sections were polished until the otolith core was clearly visible, and the area of the otolith sampled (i.e. micromill path) was described previously [13]. Core material typically represented otolith material accreted during the first four to six months of life, albeit some variation in drill paths and the fraction of age-0 period sampled did exist for certain taxa (e.g. Atlantic bluefin [14], albacore [15]). Nevertheless, otolith material was assumed to provide comparable data for assessing regional variation in otolith $\delta^{18}O$ and $\delta^{13}C$ even though we recognize that juvenile tuna may move away from their respective nursery areas during the first year of life.

Otolith $\delta^{18}O$ and $\delta^{13}C$ were quantified using an automated carbonate preparation device coupled to a gas chromatograph—isotope ratio mass spectrometer. A large fraction of the samples from all ocean basins was analysed on a Finnigan MAT 252 (Thermo Fisher Scientific, Inc.) at the University of Arizona. Isotope ratio measurements were calibrated based on repeated measurements of the National Bureau of Standards (NBS). Precision was typically *ca* ±0.10 (s.d.) and ±0.08 (s.d.) for otolith $\delta^{18}O$ and $\delta^{13}C$ values, respectively, and all values are reported relative to the Vienna Pee Dee Belemnite (VPDB) scale after comparison to an in-house laboratory standard calibrated to VPDB.

Otolith $\delta^{18}O$ and $\delta^{13}C$ values between species collected in the same region and year(s) were analysed using an analysis of variance (ANOVA) to determine whether congeners from the same region displayed statistically similar signatures, supporting the pooling of otolith $\delta^{18}O$ and $\delta^{13}C$ data from congeners collected in the same locations. Data for paired comparisons of tunas were available for tropical tunas from three locations: Western Equatorial Pacific Ocean (bigeye, yellowfin), Central Equatorial Pacific Ocean (bigeye, yellowfin) and Western Atlantic Ocean, Caribbean Sea (blackfin, yellowfin). One location in the Northeast

Table 1. Summary of otolith $\delta^{13}C$ and $\delta^{18}O$ values by region and sub-region for juvenile (age-0/1) tunas (*Thunnus* spp.) collected from 1998 to 2022 in the Atlantic, Pacific and Indian Oceans. Species of tuna are denoted as ALB (albacore), ABT (Atlantic bluefin), BET (bigeye), BKT (blackfin), PBT (Pacific bluefin) and YFT (yellowfin). Codes refer to regions defined in supplemental material (electronic supplementary material, figure S1).

region	code	primary sub-region	*N*	species	$\delta^{13}C$	s.d.	Suess $\delta^{13}C$	s.d.	$\delta^{18}O$	s.d.
Atlantic Ocean										
temperate tunas										
Northwest Atlantic	1	Mid-Atlantic Bight	89	ABT	−8.77	0.52	−9.45	0.52	−1.26	0.31
Northeast Atlantic	2	Bay of Biscay	124	ABT, ALB	−8.84	0.69	−9.29	0.64	−0.87	0.24
Mediterranean Sea	3	Balearic, Tyrrhenian, Aegean Seas	60	ABT	−9.48	1.05	−9.94	0.91	−1.07	0.37
tropical tunas										
Western Atlantic	4	Brazil	17	YFT	−9.57	0.50	−9.80	0.52	−1.69	0.25
Eastern Atlantic	5	Gulf of Guinea, Cape Verde	232	YFT	−9.57	0.50	−9.76	0.52	−1.69	0.25
Caribbean Sea	6	Lesser/Greater Antilles	136	BKT, YFT	−9.41	0.65	−9.67	0.55	−1.68	0.29
Gulf of Mexico	7	US waters	69	BKT, YFT	−9.80	0.56	−10.08	0.55	−1.70	0.26
Pacific Ocean										
temperate tunas										
Northeast Pacific	8	California, Washington	19	ALB	−8.01	0.44	−8.39	0.42	−1.22	0.37
Northwest Pacific	9	Sea of Japan, East China Sea	200	PBT	−10.44	0.61	−10.71	0.61	−2.50	0.31
tropical tunas										
Western Pacific	10	Celebes, Sulu Seas	65	BET, YFT	−10.16	0.56	−10.61	0.58	−2.65	0.21
Central Pacific >18° lat.	11	Hawaiian Islands, Cross Seamounts	137	BET, YFT	−9.78	0.44	−10.27	0.44	−1.91	0.24
Central Pacific 0–18° lat.	12	Line Islands, French Polynesia	179	BET, YFT	−9.67	0.49	−10.13	0.49	−2.15	0.34
Eastern Pacific 0–18° lat.	13	Galapagos Islands, Colombia	53	BET, YFT	−10.27	0.54	−10.29	0.53	−2.81	0.30
Eastern Pacific >18° lat.	14	Mexico, Cabo	41	YFT	−9.78	0.55	−10.07	0.53	−2.58	0.40
Indian Ocean										
tropical tunas										
Western Indian	15	Madagascar, Maldives, Seychelles	123	YFT	−10.32	0.53	−10.44	0.53	−1.87	0.32
Eastern Indian	16	Indonesia (Celebes Sea)	43	YFT	−11.13	0.43	−11.26	0.43	−2.56	0.30
total			1587							

Atlantic Ocean was available for contrasting temperate tunas (albacore, Atlantic bluefin). Paired comparisons of tropical tunas in all three locations were limited to age-0 tunas to limit the influence of movements on resulting $\delta^{18}O$ and $\delta^{13}C$ values for collections from the same location. Age-1 (12+ months) individuals were also included in a paired comparison of temperate tunas (albacore, Atlantic bluefin) from the Northeast Atlantic Ocean (Bay of Biscay) because age-0 individuals of both species in temperate nurseries are uncommon.

Otolith $\delta^{13}C$ data were adjusted for observed temporal shifts reported in previous studies, most notably the Suess effect that has resulted in a significant depletion of atmospheric ^{13}C and other carbon reservoirs (e.g. oceans) due to increased carbon dioxide (CO_2) emissions, resulting in reductions in seawater and otolith $\delta^{13}C$ content [28–30]. It is important to note that while the Suess effect is assumed to be a primary driver of reductions in otolith $\delta^{13}C$ over the period investigated, other factors such as increasing temperatures or food availability may lead to higher metabolic rates, which will also lower $\delta^{13}C$ in otoliths [31]. All otolith $\delta^{13}C$ data were standardized to 2022 (age-0 period) for global mapping projections and $\delta^{13}C$ Suess adjustments were based on an observed significant depletion rate of 0.033‰ per year for all age-0 tuna over the period examined (ANOVA $p < 0.001$; figure 1). In accordance with other studies reporting temporal variation in otolith $\delta^{18}O$ across the years being trivial [30,32], an insignificant change in otolith $\delta^{18}O$ of 0.0004‰ per year was observed for cohorts of age-0 tuna in our sample (ANOVA $p > 0.05$), and therefore, no adjustments were made to otolith $\delta^{18}O$ values for age-0/1 cohorts of tuna across the period investigated.

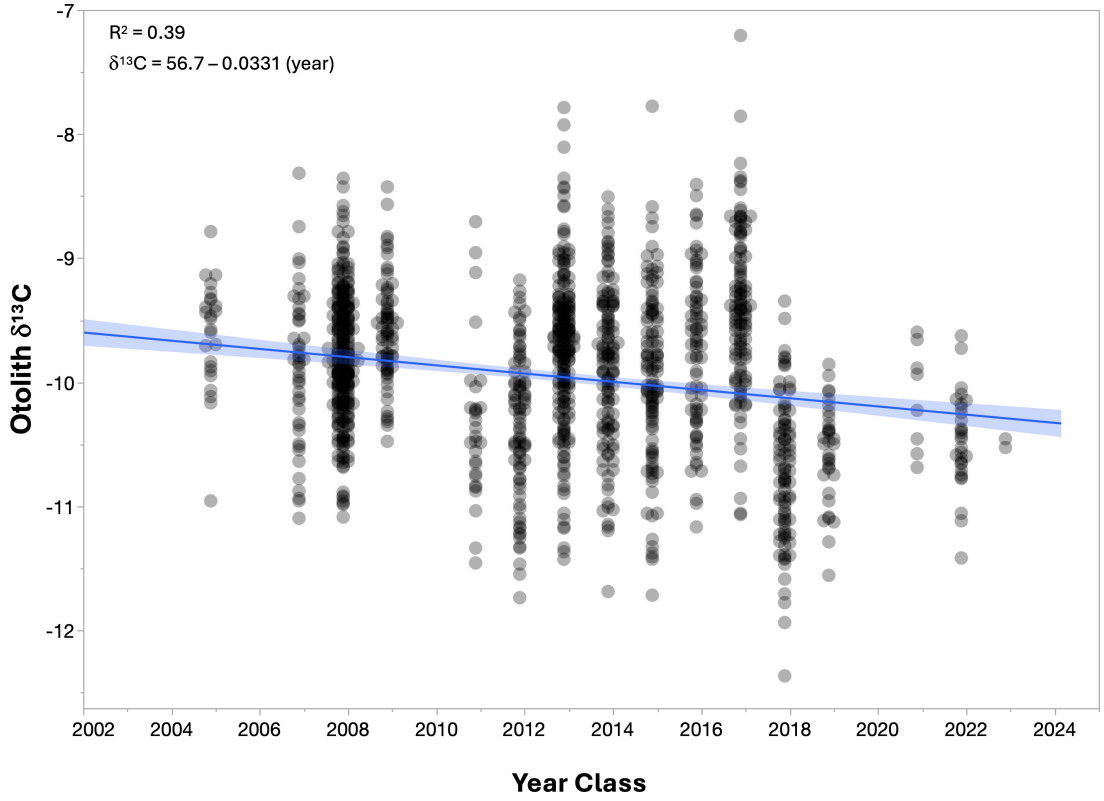

Figure 1. Otolith $\delta^{13}C$ values of age-0 tunas (*Thunnus* spp.) as a function of year class (birth year) for all geographic locations sampled. Linear regression with a 95% confidence interval is shown.

Otolith $\delta^{18}O$ and $\delta^{13}C$ isoscapes were generated in ArcGIS Pro 3.3.2 software, with data visualized as colour-shaded heat maps using inverse distance weighting (IDW) interpolation and a focal statistics function to create a continuous raster surface from discrete data points [33]. A 5° × 5° fishnet grid was overlaid on the $\delta^{18}O$ and $\delta^{13}C$ isoscapes, and the values within each cell were averaged using a spatial join function. Seawater $\delta^{18}O$ data obtained from the global seawater oxygen-18 database [34] available through the NASA Goddard Institute for Space Studies was also averaged for 5° × 5° cells with matching otolith $\delta^{18}O$ values. Mean values from within 5° × 5° grid cells that contained both otolith $\delta^{18}O$ or seawater $\delta^{18}O$ values were then used to estimate differences between the two measures of $\delta^{18}O$. In total, 30 paired 5° × 5° cells with otolith $\delta^{18}O$ and seawater $\delta^{18}O$ values were available for further analysis (electronic supplementary material, table S2).

Niche breadth of tunas based on otolith $\delta^{18}O$ and $\delta^{13}C$ values of individuals was quantified for each of the 16 major geographic regions sampled (electronic supplementary material, figure S1). Standard ellipse areas corrected for sample size (SEAc) were estimated using the Stable Isotope Bayesian Ellipses in R (SIBER) package [35] (v. 2.1.9) and used to approximate niche breadth of tunas from each region. Standard ellipse areas were generated from Bayesian multivariate normal distributions (based on 10 000 iterations) and reported as incremental Bayesian credible intervals (50%, 75% and 95%) along with the estimated mode.

3. Results

Overall, differences in otolith $\delta^{18}O$ between species pairs of age-0 tropical tunas or age-0/1 temperate tunas in spatially discrete regions in both the Atlantic Ocean and Pacific Ocean were negligible (figure 2). In paired comparisons of tuna species for all four geographic sub-regions investigated, mean otolith $\delta^{18}O$ values were statistically similar between juveniles (ANOVA, $p > 0.05$): Atlantic, Bay of Biscay (albacore [−0.74], Atlantic bluefin [−0.84]), Atlantic, Caribbean Sea (blackfin [−1.73], yellowfin [−1.71]), Pacific, Hawaiian Islands (bigeye [−1.87], yellowfin [−1.77]) and Pacific, Celebes/Sulu Seas (bigeye [−2.65], yellowfin [−2.65]). Variation in otolith $\delta^{13}C$ values of age-0 tuna between paired congeners from the same sub-region was more noticeable, with mean differences ranging from approximately 0.3‰ for paired congeners in the Caribbean Sea and Hawaiian Islands and approximately 0.5‰ between species pairs from either the Bay of Biscay or Celebes/Sulu Seas. Given that otolith $\delta^{18}O$ aligns well with ambient conditions (seawater $\delta^{18}O$) and is typically the most influential stable isotope marker for regional discrimination of pelagic fishes, our assessment of inter- and intra-ocean variability in otolith $\delta^{18}O$ as well as $\delta^{13}C$ was based on pooling congeners from a region to improve overall spatial coverage.

Large-scale inter-ocean differences in otolith $\delta^{18}O$ were observed for juvenile (age-0/1) tunas across the three oceans and 16 regions investigated (table 1), with consistently higher $\delta^{18}O$ values present for most regions in the Atlantic Ocean relative to regions in the Pacific Ocean and Indian Ocean (figure 3). Notable intra-ocean differences in otolith $\delta^{18}O$ were also observed, with the most noticeable disparity between tunas from tropical and temperate waters (figure 4A). In the Atlantic Ocean, mean otolith $\delta^{18}O$ values for temperate tunas (albacore, Atlantic bluefin) were relatively similar among the three regions sampled

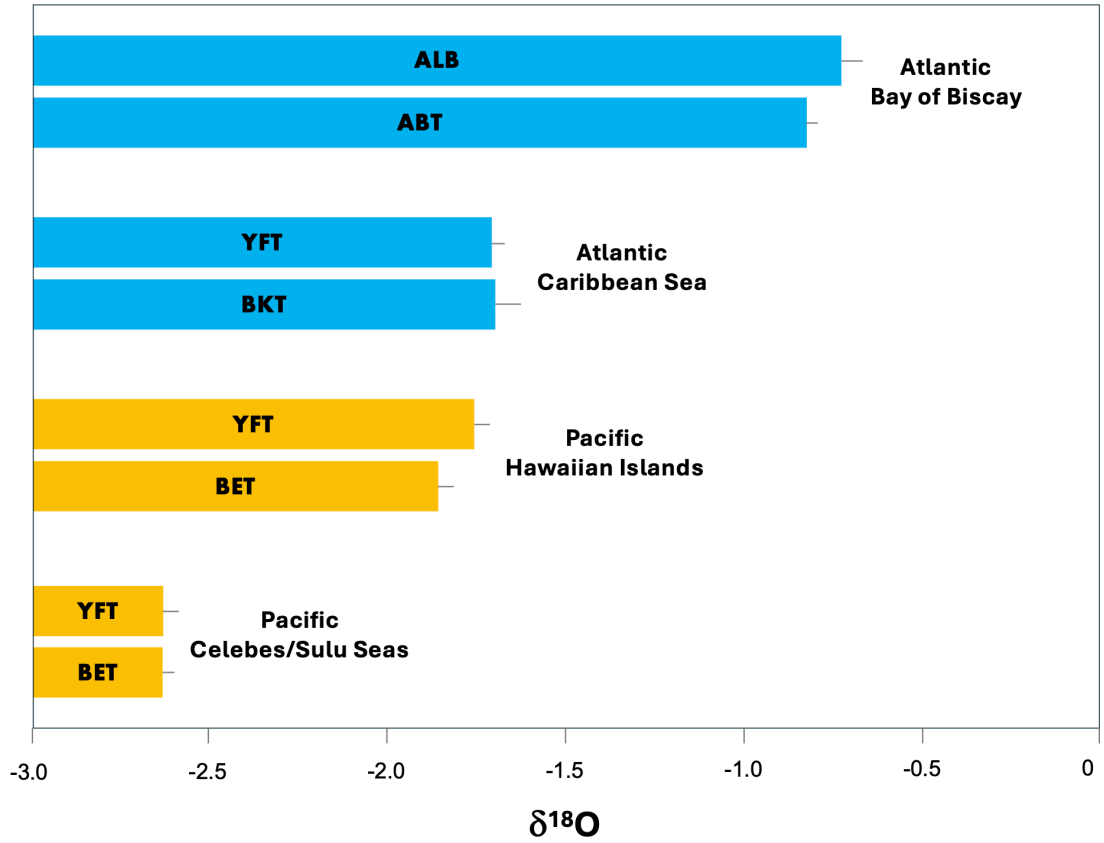

Figure 2. Mean otolith $\delta^{18}O$ of juvenile (age-0/1) tunas (*Thunnus* spp.) collected in four geographic locations in the Atlantic Ocean (blue) and Pacific Ocean (orange). Paired species from each region were used to determine whether congeners displayed similar otolith $\delta^{18}O$ values. Species of tuna are denoted as ALB (albacore), ABT (Atlantic bluefin), BET (bigeye), BKT (blackfin) and YFT (yellowfin).

with otoliths enriched in ^{18}O relative to their tropical congeners: Northeast Atlantic (−1.26‰), Mediterranean Sea (−1.07‰) and Northwest Atlantic (−0.87‰) (table 1, figure 4A). In contrast to tunas collected at higher latitudes, otolith $\delta^{18}O$ of tropical tunas (bigeye, blackfin and yellowfin) in the Atlantic Ocean were markedly depleted in ^{18}O relative to temperate tunas but nearly identical across all four regions investigated, with mean values only differing by 0.02‰: Gulf of Mexico (−1.70‰), Western Atlantic (−1.69‰), Eastern Atlantic (−1.69‰) and Caribbean Sea (−1.68‰). In the Pacific Ocean, a similar trend of higher otolith $\delta^{18}O$ values was observed for temperate tunas in the Northeast Pacific for samples collected in the California Current Large Marine Ecosystem (CCLME) (−1.22‰) relative to mean values for all five collection areas for tropical tunas in the Pacific Ocean (range: −1.91‰ to −2.81‰). Mean otolith $\delta^{18}O$ values of tropical tunas were typically lower for regions in equatorial waters, including the Western Pacific (Celebes/Sulu Seas; −2.65‰) and Eastern Pacific (Galapagos Islands/Colombia; −2.81‰), while values increased markedly (i.e. less negative) for tunas collected in the Hawaiian Islands (−1.91‰). Interestingly, mean values in the Northwest Pacific for a temperate tuna (Pacific bluefin) collected in the Sea of Japan and East China Sea were also depleted in ^{18}O (−2.50‰) and comparable with values observed for tropical tunas. In the Indian Ocean, mean otolith $\delta^{18}O$ values for the one species collected (yellowfin) were lower in the eastern region (−2.56‰) relative to the western region (−1.87‰).

Inter-ocean variation in otolith $\delta^{13}C$ of juvenile tunas was less pronounced among the three oceans, although higher $\delta^{13}C$ values were observed for several regions in the Atlantic Ocean relative to regions in the Pacific Ocean (figure 3). Intra-ocean trends in otolith $\delta^{13}C$ were not as distinct or as consistent as trends observed for otolith $\delta^{18}O$, but an eastern to western gradient in otolith $\delta^{13}C$ was evident for regions in temperate and/or tropical zones in certain oceans (figure 4B). In the Atlantic Ocean, mean otolith $\delta^{13}C$ values for temperate tunas (albacore, Atlantic bluefin) between the Northeast and Northwest regions were nearly identical (raw: −8.84‰ and −8.77‰; Suess-adjusted −9.29‰ and −9.45‰, respectively) (table 1, figure 4B). In contrast, otolith $\delta^{13}C$ of a temperate tuna (Atlantic bluefin) from the Mediterranean Sea displayed values approximately 0.4‰ lower than the Northeast and Northwest regions in the Atlantic Ocean (raw: −9.48‰; Suess-adjusted −9.94‰). For tropical tunas (blackfin, yellowfin) collected from four different regions of the Atlantic Ocean, mean otolith $\delta^{13}C$ values were depleted in ^{13}C relative to temperate tunas for both raw (−9.41‰ to −9.80‰) and Suess-adjusted (−9.67‰ to −10.08‰) values. For temperate tunas in the Pacific Ocean (albacore, Pacific bluefin), otolith $\delta^{13}C$ values were markedly different, with mean values showing greater than a 2.0‰ shift between the Northeast Pacific (raw: −8.01‰, Suess-adjusted −8.39‰) and Northwest Pacific (raw: −10.44‰, Suess-adjusted −10.71‰). For tropical tunas in the Pacific Ocean (bigeye, yellowfin), otolith $\delta^{13}C$ values varied moderately among the five regions sampled (raw −9.67‰ to −10.27‰, Suess-adjusted −10.07‰ to −10.61‰), with values depleted by approximately 0.3–0.4‰ relative to tropical tunas sampled in the Atlantic Ocean. Otolith $\delta^{13}C$ for one species of tropical tuna (yellowfin) from the Indian Ocean was higher in the western region (raw: −10.32‰, Suess-adjusted −10.44‰) relative to the eastern region (raw: −11.13‰, Suess-adjusted −11.26‰). Both raw and Suess-adjusted otolith $\delta^{13}C$ values for tuna from the eastern Indian Ocean indicated that otoliths from this region were more depleted in ^{13}C than all other regions investigated.

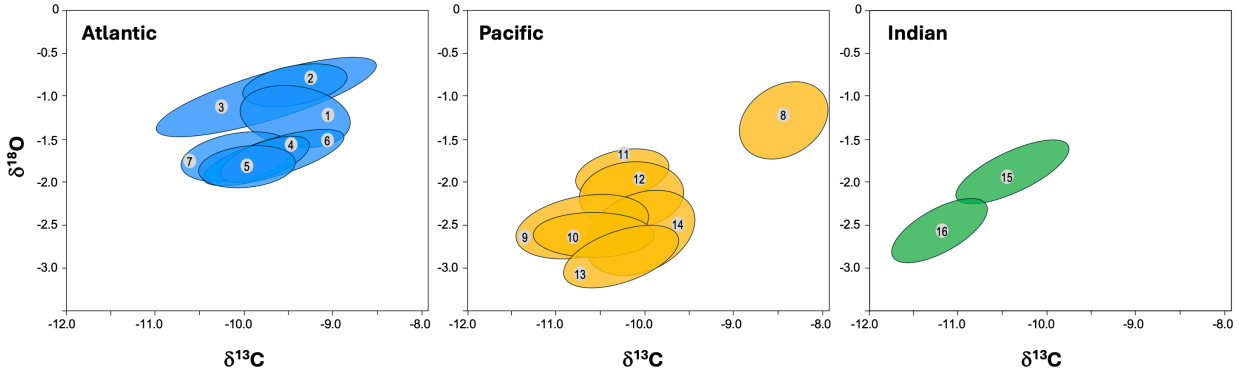

Figure 3. Fifty per cent confidence ellipses based on otolith $\delta^{18}O$ and $\delta^{13}C$ values for juvenile (age-0/1) tunas (*Thunnus* spp.) from the Atlantic Ocean (regions 1–7, blue), Pacific Ocean (regions 8–14, orange) and Indian Ocean (regions 15,16, green). Description of region codes provided in table 1.

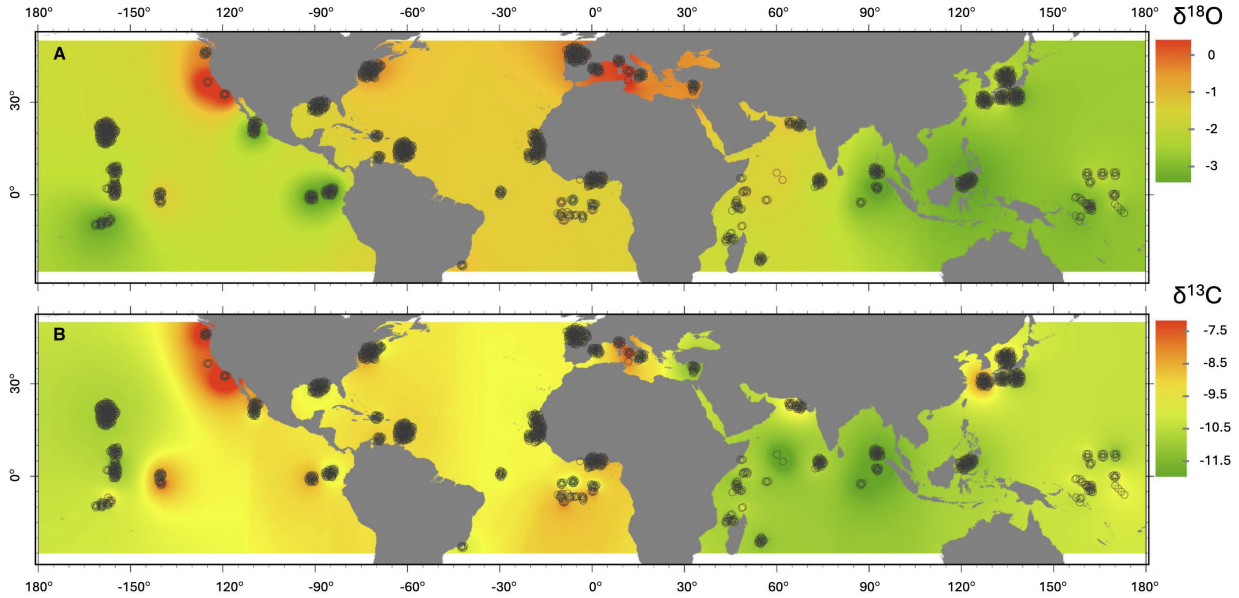

Figure 4. Otolith (A) $\delta^{18}O$ and (B) $\delta^{13}C$ isoscapes for juvenile (age-0/1) tunas (*Thunnus* spp.) based on individuals collected (open black circles) in the Atlantic Ocean, Pacific Ocean and Indian Ocean. Isoscapes derived with inverse distance weighting interpolation and smoothing functions.

Niche breadth based on otolith $\delta^{18}O$ and $\delta^{13}C$ values of juvenile tunas and expressed as SEAc was highly variable across the 16 regions sampled; however, differences between temperate and tropical tunas were observed along with similarities in SEAc for tropical tunas from different regions within the same ocean basin (figure 5). In the Atlantic Ocean, SEAc values were typically higher for temperate tunas compared with tropical tunas, and the largest niche breadth was present for individuals (entirely Atlantic bluefin) collected in the Mediterranean Sea (mode: 0.72‰^{2}). Niche breadth of tropical tunas collected from three regions in the Atlantic Ocean (Eastern Atlantic, Caribbean Sea, Gulf of Mexico) was narrower and highly similar, with SEAc modes all within 0.02‰ of each other (0.42‰^{2} to 0.44‰^{2}). The lowest SEAc for tropical tunas was observed for individuals collected in equatorial waters off Brazil (0.29‰^{2}), the southernmost region sampled in the Atlantic Ocean. No conspicuous tropical versus temperate trend in niche breadth was present for regions sampled in the Pacific Ocean, albeit three of the lowest SEAc (0.30‰^{2} to 0.42‰^{2}) were observed for regions with tropical tunas (Western Pacific, Central Pacific greater than 18° latitude, Eastern Pacific 0–18° latitude), with niche breadth in the two other tropical regions in the Pacific Ocean approximately 0.1–0.2‰^{2} greater. Individuals collected from the western and eastern regions of the Indian Ocean displayed similar SEAc values (0.36‰^{2} and 0.32‰^{2}, respectively) that were generally comparable with values observed for tropical tunas collected from most regions in both the Atlantic Ocean and Pacific Ocean. Interestingly, the degree of natural variability in niche breadth denoted by the range of Bayesian credible intervals (50%, 75% and 95%) was highest for three regions (Mediterranean Sea, Northeast Pacific and Eastern Pacific greater than 18°N), and all three comprised a single species of tuna, suggesting that observed increases in niche breadth were not a function of mixed-species assemblages of *Thunnus* in a given region.

4. Discussion

Juvenile (age-0/1) tunas from the same regions and collection periods displayed nearly equivalent otolith $\delta^{18}O$ values and, to a lesser degree, similar trends in otolith $\delta^{13}C$ values, suggesting that congeners at the spatial scale (i.e. region) investigated probably resided in these regions for a sufficient period of time to reflect baseline or ambient $\delta^{18}O$ and $\delta^{13}C$ conditions. Our findings of comparable otolith $\delta^{18}O$ and $\delta^{13}C$ values in paired age-0 tropical tunas collected from the same region and time

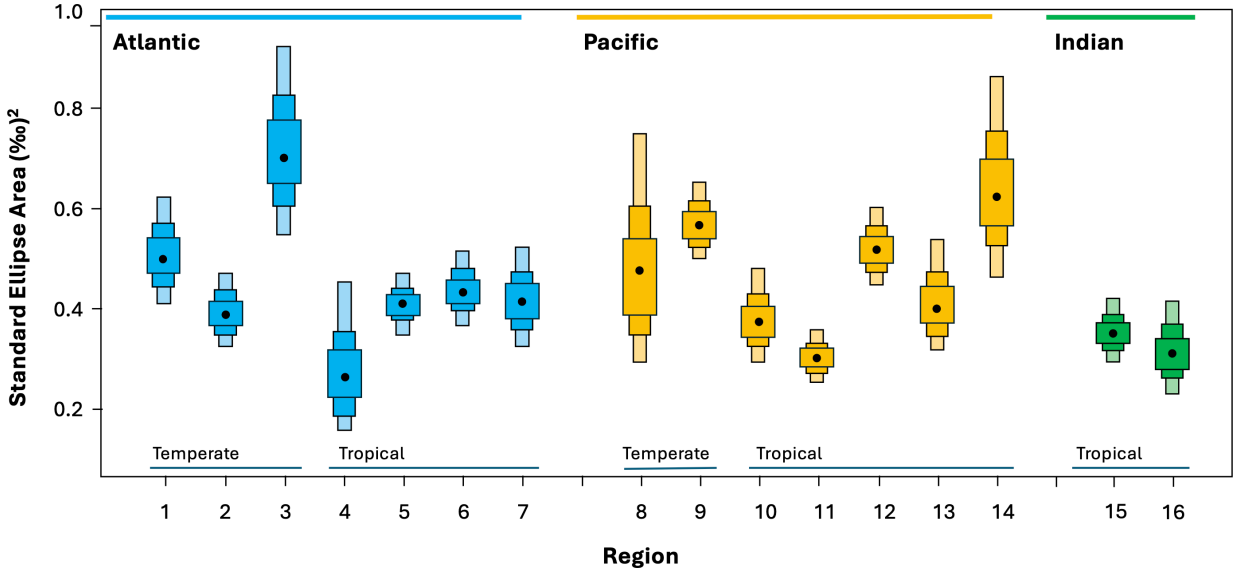

Figure 5. Standard ellipse area (SEAc) density plots of otolith $\delta^{18}O$ and $\delta^{13}C$ for juvenile (age-0/1) tunas (*Thunnus* spp.) from the Atlantic Ocean (regions 1–7, blue), Pacific Ocean (regions 8–14, orange) and Indian Ocean (regions 15,16, green). Description of region codes provided in table 1. Regions with tropical and temperate tunas denoted. Black dots (•) represent the SEAc mode for each region, and shaded boxes represent incremental Bayesian credible intervals from darkest to lightest: 50%, 75% and 95%.

are in accord with other studies reporting similar isotopic signatures between congeners of juvenile fishes that co-occur within the same ecosystem [18]. Moreover, studies quantifying $\delta^{18}O$ and $\delta^{13}C$ in other biogenic carbonates have reported comparable values between congeneric species collected in the same habitat or area [36]. Consequently, results support the premise that otolith $\delta^{18}O$ and $\delta^{13}C$ values of co-occurring congeners in the genus *Thunnus* are ostensibly suitable for developing region-specific otolith $\delta^{18}O$ and $\delta^{13}C$ markers that can be used to address questions related to their origin and population connectivity; however, we recognize that differential residency periods and migration patterns of congeners prior to capture may lead to greater isotopic variability within a region [22].

Inter- and intra-ocean trends in otolith $\delta^{18}O$ values of juvenile (age-0/1) tunas were evident in the Atlantic, Pacific and Indian Oceans. Tunas from several regions in the Atlantic Ocean commonly display higher otolith $\delta^{18}O$ values than counterparts in tropical and/or temperate zones in the Pacific and Indian Oceans. For juveniles in all three ocean basins, regional variability in otolith $\delta^{18}O$ values was evident, but at the same time, this marker was relatively similar across regions within tropical zones in both oceans. Observed regional and ocean basin differences in otolith $\delta^{18}O$ followed well-established patterns reported for seawater $\delta^{18}O$ [25,34,37]; however, otolith $\delta^{18}O$ was approximately 2.3‰ lower than seawater $\delta^{18}O$ (based on mean difference for 30 paired samples in 5° × 5° cells with both otolith and seawater $\delta^{18}O$ measurements; electronic supplementary material, table S2). Analogous to seawater $\delta^{18}O$, otolith $\delta^{18}O$ values of tunas generally declined at lower latitudes, with temperate tunas (i.e. albacore, Atlantic and Pacific bluefin) exposed to lower sea surface temperatures (SST) displaying elevated otolith $\delta^{18}O$ values (enriched in ^{18}O) relative to congeners in tropical waters (bigeye, blackfin and yellowfin). Our finding of depleted otolith ^{18}O with increasing SST from temperate to tropical zones matches a well-documented inverse relationship between SST and otolith $\delta^{18}O$ due to temperature-dependent fractionation [38–40]. The apparent SST-driven, latitudinal gradient in otolith $\delta^{18}O$ for tunas from temperate and tropical regions was observed in both the Atlantic and Pacific Oceans. It is important to note that physiological effects (kinetic or metabolic) influence temperature-$\delta^{18}O$ fractionation, and thus these vital processes may also influence otolith $\delta^{18}O$, although previous studies suggest that ambient SST largely controls otolith $\delta^{18}O$ [41].

Seawater $\delta^{18}O$ values are positively correlated with salinity [42,43], and we also observed correlation between otolith $\delta^{18}O$ and salinity within and across ocean basins. Higher salinity and seawater $\delta^{18}O$ values are characteristic of regions with higher evaporation, which disproportionately leaves more of the heavier isotope (^{18}O) in seawater. Conversely, areas with freshwater inflow (lower salinity) maintain lower seawater $\delta^{18}O$ due to freshwater originating from the atmosphere (precipitation) being isotopically lighter than seawater [26]. At the ocean-basin scale, average sea surface salinity of regions sampled for tropical tunas in the Pacific Ocean was approximately 2 practical salinity units (psu) lower than tropical waters in the Atlantic Ocean. Corresponding shifts in region-specific means in otolith $\delta^{18}O$ values for tropical tunas followed the expected pattern with elevated values for tropical tunas in the more saline Atlantic Ocean (−1.70‰ to −1.68‰) relative to the Pacific Ocean (−2.65‰ to −1.90‰). Differences in otolith $\delta^{18}O$ of tunas from two marginal seas in the Atlantic Ocean also support this positive salinity-seawater $\delta^{18}O$ relationship, with more positive otolith $\delta^{18}O$ values for juvenile tunas from the Mediterranean Sea (*ca* −1.1‰), where evaporation and salinity are elevated (mean salinity approx. 38–40) compared with tunas from the northern Gulf of Mexico (−1.7‰), which is characterized by higher freshwater inflow and lower salinity (mean approx. 34–36). Interestingly, the Gulf of Mexico and Mediterranean Sea represent critical spawning areas of Atlantic bluefin tuna, and the observed differences in otolith $\delta^{18}O$ between the two marginal seas have been used previously to predict the natal origin and trans-Atlantic migration patterns of this species [8,24].

To date, studies investigating ocean-scale patterns in $\delta^{13}C$ have centred on values of particulate organic matter (POM) as a proxy for phytoplankton or primary consumers (i.e. zooplankton) [25,44,45]. Characterizations of spatial trends in otolith

$\delta^{13}C$ values and other biogenic carbonates at the ocean-basin scale are lacking. The development of otolith $\delta^{13}C$ isoscapes has received less attention due primarily to the fact that cosmopolitan distributions of juveniles from a single species or complex of species are rare. Moreover, resulting $\delta^{13}C$ values are not simple reflections of ambient physico-chemical conditions (e.g. temperature, salinity), but the result of complex interactions among several factors (biological, kinetic and thermodynamic) [31,46], which limits their ability to serve as region-specific markers. Moreover, seasonal shifts in baseline $\delta^{13}C$ values of producer signatures (i.e. POM) or primary consumers (zooplankton) that transfer organic matter to higher order consumers (tunas) can change seasonally by 2–3‰ at the same location [47–49], further limiting the value of $\delta^{13}C$ for regional discrimination. We also observed a prominent temporal decline in otolith $\delta^{13}C$ values of juvenile tunas (0.033‰ reduction per year) across the two-decade sampling scheme used in this study, which is attributed to the depletion of atmospheric ^{13}C due to fossil fuel emissions or the Suess effect [29,30]. Together, these factors complicate the interpretation of otolith $\delta^{13}C$ because, unlike $\delta^{18}O$ that is deposited at near equilibrium with seawater, dietary carbon from prey along with dissolved inorganic carbon (DIC) contribute to the otolith $\delta^{13}C$ value [50].

Suess-adjusted otolith $\delta^{13}C$ values of tunas followed expected trends at the regional and ocean-basin scales. Specifically, we observed distinct gradients of increasing otolith $\delta^{13}C$ moving from lower to higher latitudes, with otoliths more enriched in ^{13}C for temperate tunas (albacore, Atlantic and Pacific bluefin) collected at higher latitudes with lower SST relative to tropical tunas in the same ocean basin. Again, decreasing SST moving from lower (warmer) to higher (cooler) latitudes was observed for tunas, aligning with previous research demonstrating that higher SST resulted in more depleted ^{13}C in phytoplankton [51,52]. Given that only a small proportion of otolith carbon is derived from the diet, increased metabolic rate driven by higher SST is believed to play a larger role than SST effects on phytoplankton itself, leading to lower otolith $\delta^{13}C$ by increasing the contribution of dietary carbon to the otolith [31]. Longitudinal trends in both SST and otolith $\delta^{13}C$ further underscore this relationship with the observation that tunas collected from the two regions with the highest average SST [53], Western Pacific and Eastern Indian Ocean, displayed the lowest otolith $\delta^{13}C$ values (approx. −10.7‰) of all regions assayed. Apart from the temperature-related influence, regions with elevated nutrients and higher primary productivity (i.e. upwelling zones) are known to show ^{13}C enrichment [25,54,55], elevating baseline values of $\delta^{13}C$ in phytoplankton. Similarly, tunas collected in notable upwelling areas in the Northeast Pacific Ocean off California (CCLME) and the Northeast Atlantic in the Bay of Biscay were characterized by elevated otolith $\delta^{13}C$ values (−8.39‰ and −9.29‰, respectively) relative to juvenile tunas from other regions sampled within each ocean basin.

Quantification of niche breadth using otolith $\delta^{18}O$ and $\delta^{13}C$ values of tunas was variable across regions and ocean basins, but often similar for tunas collected within tropical or temperate zones. We also observed that regions and species found to have wider niche breadth were often at higher latitudes where individuals probably experienced more variable environmental conditions. This aligns well with ecological niche theory, where increased environmental heterogeneity or fluctuating environmental conditions experienced by individuals leads to wider niche breadth [56]. Studies have also demonstrated that temporal variation in environmental conditions experienced by individuals may be a more important determinant of niche breadth than other spatial factors [57,58]. Therefore, it is reasonable to assume that temperate tunas from higher-latitude ecosystems with more variable biological and physico-chemical conditions (e.g. SST) may lead to wider niche breadth (larger SEAc) compared with their tropical tuna counterparts. The estimated niche breadth of temperate and tropical tunas across the 16 regions supports this premise, with the narrowest observed SEAc present for tropical tunas from several regions, while the two largest SEAc values were observed for tunas in temperate regions. While increased variability in environmental conditions probably contributed to increased niche breadth of temperate tunas, it is important to note that our samples in the two regions with the largest SEAc included age-1 fish. Observed $\delta^{18}O$ and $\delta^{13}C$ values for certain age-1 fish were based on otolith material that covered longer lifetime periods (i.e. entire first year of life) and therefore may reflect longer and more variable exposure periods. We also observed an elevated SEAc for yellowfin tuna in the Eastern Pacific Ocean at latitudes greater than 18°N, and increased niche breadth for tunas in this region may be due to complex circulation and seasonally variable oceanographic conditions linked to the convergence of several warm and cold currents in this region (equatorial counter current, California current, Costa Rica current [59]). Finally, it is plausible to assume that the inclusion of more than one species within a region will artificially inflate estimated niche breadth based on SEAc; however, all three regions with the highest observed SEAc comprised a single species of *Thunnus*, while many regions with lower SEAc comprised more than one species, suggesting mixed-species assemblages of congeners did not appear to bias our niche breadth estimates.

Despite their promise, caveats and/or limitations are associated with using otolith $\delta^{18}O$ and $\delta^{13}C$ values to address questions related to migrations and population connectivity of tunas since they are capable of traversing multiple ecosystems or regions during the first year(s) of life [10]. Consequently, otolith $\delta^{18}O$ and $\delta^{13}C$ values of individuals in our samples of over 1500 juvenile tunas represent integrated values for each fish that reflect both biological and physiochemical conditions or processes across all regions inhabited during the period of the otolith sampled. Spatial and temporal shifts in the distribution of individuals and associated changes in ocean conditions at each location further complicate the application and interpretation of otolith $\delta^{18}O$ and $\delta^{13}C$ values as region-specific markers for understanding metapopulation structure [14]. Moreover, regions or areas of interest for a species (e.g. spawning, nursery or foraging zones) may not be distinct geochemically, as demonstrated for regions in both the tropical Atlantic Ocean (Caribbean Sea and Gulf of Mexico) and tropical Pacific Ocean (Eastern Pacific and Central Pacific greater than 18°N), limiting the value of $\delta^{18}O$ and $\delta^{13}C$ for discriminating individuals between certain regions [13,19].

5. Conclusions

Geochemical markers in otoliths—including $\delta^{18}O$ and $\delta^{13}C$—provide valuable information regarding the natal origin, migration patterns and stock mixing of tunas at the ocean-basin scale. By integrating new otolith $\delta^{18}O$ and $\delta^{13}C$ data with previously published data, distinct inter- and intra-ocean trends were detected, and resulting otolith $\delta^{18}O$ and $\delta^{13}C$ isoscapes will serve as global baselines for assessing the utility of these natural tags for future investigations of tropical and temperate tunas at different spatial scales in pelagic ecosystems. Because otolith $\delta^{18}O$ and $\delta^{13}C$ signatures are reflective of niche parameters (e.g. resource use, diet and ambient physico-chemical conditions), these geochemical markers also show considerable promise for exploring the ecological niche dynamics of tunas and other highly migratory species in pelagic ecosystems.

Ethics. All collections were performed in accordance with relevant guidelines and regulations of institutional animal welfare committee.

Data accessibility. All otolith $\delta^{18}O$ and $\delta^{13}C$ data provided in supplementary materials.

Supplementary material is available online [60].

Declaration of AI use. We have not used AI-assisted technologies in creating this article.

Authors' contributions. J.R.R.: conceptualization, data curation, formal analysis, funding acquisition, investigation, project administration, visualization, writing—original draft; R.J.D.W.: conceptualization, data curation, investigation, writing—review and editing; I.A.-A.: conceptualization, data curation, investigation, writing—review and editing; H.A.: data curation, investigation, writing—review and editing; I.F.: conceptualization, data curation, investigation, writing—review and editing; M.A.D.: investigation, writing—review and editing; P.L.L.: investigation, writing—review and editing; L.M.: investigation, writing—review and editing; A.P.: data curation, investigation, writing—review and editing; S.A.S.: investigation, writing—review and editing; N.W.: formal analysis, writing—review and editing; M.Z.S.: data curation, writing—review and editing.

All authors gave final approval for publication and agreed to be held accountable for the work performed therein.

Conflict of interest declaration. We declare we have no competing interests.

Funding. Analysis and development of the manuscript was supported by the Gulf Research Institute for Highly Migratory Species (GRIHMS), the McDaniel Charitable Foundation and Texas A&M University. Otolith collections used in the meta-analysis were obtained from a variety of projects and sources with financial assistance from the Basque Government, ICCAT's Atlantic Wide Research Program for Bluefin Tuna (GBYP), NOAA Fisheries, FAO/IOTC, GRIHMS and other entities.

Acknowledgements. We are grateful to the large network of scientists involved with the collection of otolith samples from juvenile tunas. A special thanks to key personnel who were critical to sampling efforts over the years: D. Itano, B. Falterman, T. Itoh, L. Kitchens, P. Addis, A. Corriero, G. DeMetrio, H. Dewar, S. Karakulak, P. Megalofonou, H. Murua, S. Ohshimo, L. Reynal, E. Saillant, D. Secor, O. Snodgrass, Y. Tanaka, and V. Ticina. We are also thankful to the commercial and artisanal fishers that assisted with collections.

References

1. Hammerschlag N *et al*. 2019 Ecosystem function and services of aquatic predators in the anthropocene. *Trends Ecol. Evol*. **34**, 369–383. (doi:10.1016/j.tree.2019.01.005)
2. Baum JK, Worm B. 2009 Cascading top-down effects of changing oceanic predator abundances. *J. Appl. Ecol*. **78**, 699–714. (doi:10.1111/j.1365-2656.2009.01531.x)
3. Harrison AL *et al*. 2018 The political biogeography of migratory marine predators. *Nat. Ecol. Evol*. **2**, 1571–1578. (doi:10.31230/osf.io/3p4eb)
4. Rooker JR *et al*. 2019 Population connectivity of pelagic megafauna in the Cuba-Mexico-United States triangle. *Sci. Rep*. **9**, 1663. (doi:10.1038/s41598-018-38144-8)
5. Block BA *et al*. 2011 Tracking apex marine predator movements in a dynamic ocean. *Nature* **475**, 86–90. (doi:10.1038/nature10082)
6. Rodríguez-Ezpeleta N. 2019 Genetic assignment of Atlantic bluefin tuna natal origin: a new tool for improved management. *Front. Ecol. Env.* **17**, 439–444. (doi:10.1002/fee.2090)
7. Relano V, Pauly D. 2022 Philopatry as a tool to define tentative closed migration cycles and conservation areas for large pelagic fishes in the Pacific. *Sustainability* **14**, 5577. (doi:10.3390/su14095577)
8. Rooker JR, Secor DH, De Metrio G, Schloesser R, Block BA, Neilson JD. 2008 Natal homing and connectivity in Atlantic bluefin tuna populations. *Science* **322**, 742–744. (doi:10.1126/science.1161473)
9. Madigan DJ, Baumann Z, Carlisle AB, Hoen DK, Popp BN, Dewar H, Snodgrass OE, Block BA, Fisher NS. 2014 Reconstructing transoceanic migration patterns of Pacific bluefin tuna using a chemical tracer toolbox. *Ecology* **95**, 1674–1683. (doi:10.1890/13-1467.1)
10. Rooker JR *et al*. 2023 Nursery origin of yellowfin tuna in the western Atlantic Ocean: significance of Caribbean Sea and trans-Atlantic migrants. *Sci. Rep*. **13**, 16277. (doi:10.1038/s41598-023-43163-1)
11. Rooker J *et al*. 2014 Crossing the line: migratory and homing behaviors of Atlantic bluefin tuna. *Mar. Ecol. Prog. Ser*. **504**, 265–276. (doi:10.3354/meps10781)
12. Fraile I, Arrizabalaga H, Rooker JR. 2015 Origin of Atlantic bluefin tuna (*Thunnus thynnus*) in the Bay of Biscay. *ICES J. Mar. Sci*. **72**, 625–634. (doi:10.1093/icesjms/fsu156)
13. Kitchens L, Rooker J, Reynal L, Falterman B, Saillant E, Murua H. 2018 Discriminating among yellowfin tuna *Thunnus albacares* nursery areas in the Atlantic Ocean using otolith chemistry. *Mar. Ecol. Prog. Ser*. **603**, 201–213. (doi:10.3354/meps12676)
14. Rooker S JR, Secor DH, DeMetrio G, Kaufman JA, Belmonte Rios A, Ticina A. 2008 Evidence of trans-Atlantic mixing and natal homing of bluefin tuna. *Mar. Ecol. Prog. Ser.* **368**, 231–239. (doi:10.3354/meps07602)
15. Fraile I, Arrizabalaga H, Santiago J, Goñi N, Arregi I, Madinabeitia S, Wells RJD, Rooker JR. 2016 Otolith chemistry as an indicator of movements of albacore (*Thunnus alalunga*) in the North Atlantic Ocean. *Mar. Freshw. Res*. **67**, 1002–1013. (doi:10.1071/MF15097)
16. Wells RJD, Kinney MJ, Kohin S, Dewar H, Rooker JR, Snodgrass OE. 2015 Natural tracers reveal population structure of albacore (*Thunnus alalunga*) in the eastern North Pacific Ocean. *ICES J. Mar. Sci*. **72**, 2118–2127. (doi:10.1093/icesjms/fsv051)
17. Rooker JR, Wells RJD, Itano DG, Thorrold SR, Lee JM. 2016 Natal origin and population connectivity of bigeye and yellowfin tuna in the Pacific Ocean. *Fish. Oceanogr*. **25**, 277–291. (doi:10.1111/fog.12154)
18. Wells RJD, Mohan JA, Dewar H, Rooker JR, Tanaka Y, Snodgrass OE, Kohin S, Miller NR, Ohshimo S. 2020 Natal origin of Pacific bluefin tuna from the California Current Large Marine Ecosystem. *Biol. Lett*. **16**, 20190878. (doi:10.1098/rsbl.2019.0878)
19. Artetxe-Arrate I, Fraile I, Clear N, Darnaude A, Dettman D, Pécheyran C, Farley J, Murua H. 2021 Discrimination of yellowfin tuna *Thunnus albacares* between nursery areas in the Indian Ocean using otolith chemistry. *Mar. Ecol. Prog. Ser*. **673**, 165–181. (doi:10.3354/meps13769)

20. Artetxe-Arrate I *et al*. 2025 Otolith stable isotopes highlight the importance of local nursery areas as the origin of recruits to yellowfin tuna (*Thunnus albacares*) fisheries in the western Indian Ocean. *Fish. Res*. **281**, 107241. (doi:10.1016/j.fishres.2024.107241)
21. Baumann H, Wells RJD, Rooker JR, Zhang S, Baumann Z, Madigan DJ, Dewar H, Snodgrass OE, Fisher NS. 2015 Combining otolith microstructure and trace elemental analyses to infer the arrival of juvenile Pacific bluefin tuna in the California current ecosystem. *ICES J. Mar. Sci*. **72**, 2128–2138. (doi:10.1093/icesjms/fsv062)
22. Rooker JR *et al*. 2021 Natal origin and age-specific egress of Pacific bluefin tuna from coastal nurseries revealed with geochemical markers. *Sci. Rep*. **11**, 14216. (doi:10.1038/s41598-021-93298-2)
23. Morse MR, Kerr LA, Galuardi B, Cadrin SX. 2020 Performance of stock assessments for mixed-population fisheries: the illustrative case of Atlantic bluefin tuna. *ICES J. Mar. Sci*. **77**, 2043–2055. (doi:10.1093/icesjms/fsaa082)
24. Rooker JR *et al*. 2019 Wide-ranging temporal variation in transoceanic movement and population mixing of bluefin tuna in the North Atlantic Ocean. *Front. Mar. Sci*. **6**, 398. (doi:10.3389/fmars.2019.00398)
25. Kerr LA, Whitener ZT, Cadrin SX, Morse MR, Secor DH, Golet W. 2020 Mixed stock origin of Atlantic bluefin tuna in the U.S. rod and reel fishery (Gulf of Maine) and implications for fisheries management. *Fish. Res*. **224**, 105461. (doi:10.1016/j.fishres.2019.105461)
26. McMahon KW, Hamady LL, Thorrold SR. 2013 A review of ecogeochemistry approaches to estimating movements of marine animals. *Limnol. Oceanogr*. **58**, 697–714. (doi:10.4319/lo.2013.58.2.0697)
27. Wells RJD, Rooker JR, Prince ED. 2010 Regional variation in the otolith chemistry of blue marlin (*Makaira nigricans*) and white marlin (*Tetrapturus albidus*) from the western North Atlantic Ocean. *Fish. Res*. **106**, 430–436. (doi:10.1016/j.fishres.2010.09.017)
28. Suess HE. 1955 Radiocarbon concentrations in modern wood. *Science* **122**, 415–417. (doi:10.1126/science.122.3166.415.b)
29. Spero HJ, Bijma J, Lea DW, Bemis BE. 1997 Effect of seawater carbonate concentration on foraminiferal carbon and oxygen isotopes. *Nature* **390**, 497–500. (doi:10.1038/37333)
30. Schloesser RW, Rooker JR, Louchuoarn P, Neilson JD, Secord DH. 2009 Interdecadal variation in seawater $\delta^{13}C$ and $\delta^{18}O$ recorded in fish otoliths. *Limnol. Oceanogr*. **54**, 1665–1668. (doi:10.4319/lo.2009.54.5.1665)
31. Chung MT, Trueman CN, Godiksen JA, Grønkjær P. 2019 Otolith $\delta^{13}C$ values as a metabolic proxy: approaches and mechanical underpinnings. *Mar. Freshw. Res*. **70**, 17471756. (doi:10.1071/mf18317)
32. Fraile I *et al*. 2016 The imprint of anthropogenic CO_2 emissions on Atlantic bluefin tuna otoliths. *J. Mar. Syst*. **158**, 26–33. (doi:10.1016/j.jmarsys.2015.12.012)
33. Wunder MB. 2010 Using isoscapes to model probability surfaces for determining geographic origins. In *Isoscapes* (eds J West, G Bowen, T Dawson, K Tu), pp. 251–270. Dordrecht, The Netherlands: Springer. (doi:10.1007/978-90-481-3354-3_12)
34. Schmidt GA, Bigg GR, Rohling EJ. 1999 *Global Seawater Oxygen-18 Database - v1.22*. See https://data.giss.nasa.gov/o18data/.
35. Jackson A, Parnell A. 2023 *SIBER: stable isotope Bayesian ellipses in R*. See https://cran.r-project.org/package=SIBER.
36. Dance MA, Bello G, Furey NB, Rooker JR. 2014 Species-specific variation in cuttlebone $\delta^{13}C$ and $\delta^{18}O$ for three species of Mediterranean cuttlefish. *Mar. Biol*. **161**, 489–494. (doi:10.1007/s00227-013-2346-x)
37. Rohling EJ. 2013 Oxygen isotope composition of seawater. In *The encyclopedia of quaternary science* (ed. SA Elias), pp. 915–922, vol. **2**. Amsterdam, The Netherlands: Elsevier. (doi:10.1016/B978-0-323-99931-1.00317-2)
38. Høie H, Otterlei E, Folkvord A. 2004 Temperature-dependent fractionation of stable oxygen isotopes in otoliths of juvenile cod (*Gadus morhua* L.). *ICES J. Mar. Sci*. **61**, 243–251. (doi:10.1016/j.icesjms.2003.11.006)
39. Kim ST, O'Neil JR, Hillaire-Marcel C, Mucci A. 2007 Oxygen isotope fractionation between synthetic aragonite and water: influence of temperature and Mg^{2+} concentration. *Geochim. et Cosmochim. Acta* **71**, 4704–4715. (doi:10.1016/j.gca.2007.04.019)
40. Trueman CN *et al*. 2023 Thermal sensitivity of field metabolic rate predicts differential futures for bluefin tuna juveniles across the Atlantic Ocean. *Nat. Commun*. **14**, 7379. (doi:10.1038/s41467-023-41930-2)
41. Graham BS, Koch PL, Newsome SD, McMahon KW, Aurioles D. 2010 Using isoscapes to trace the movements and foraging behavior of top predators in Oceanic ecosystems. In *Isoscapes* (eds JB West, GJ Bowen, TE Dawson, KP Tu), pp. 299–318. Dordrecht, The Netherlands: Springer Netherlands. (doi:10.1007/978-90-481-3354-3_14)
42. Darnaude AM, Sturrock A, Trueman CN, Mouillot D, Campana SE, Hunter E. 2014 Listening in on the past: what can otolith $\delta^{18}O$ values really tell us about the environmental history of fishes? *PLoS One* **9**, e108539. (doi:10.1371/journal.pone.0108539)
43. von Leesen G, Ninnemann US, Campana SE. 2020 Stable oxygen isotope reconstruction of temperature exposure of the Icelandic cod (*Gadus morhua*) stock over the last 100 years. *ICES J. Mar. Sci*. **10**, 1093 (doi:10.1093/icesjms/fsaa011)
44. Close HG, Henderson LC. 2020 Open-ocean minima in $\delta^{13}C$ values of particulate organic carbon in the lower euphotic zone. *Front. Mar. Sci*. **7**, 540165. (doi:10.3389/fmars.2020.540165)
45. Verwega MT, Somes CJ, Schartau M, Tuerena RE, Lorrain A, Oschlies A, Slawig T. Description of a global marine particulate organic carbon-13 isotope data set. *Earth Syst. Sci. Data* **13**, 4861–4880. (doi:10.5194/essd-2021-159)
46. Tagliabue A, Bopp L. 2008 Towards understanding global variability in ocean carbon-13. *Global Biogeochem. Cycles* **22**, GB1025. (doi:10.1029/2007GB003037)
47. Ke Z, Li R, Chen D, Zhao C, Tan Y. 2022 Spatial and seasonal variations in the stable isotope values and trophic positions of dominant zooplankton groups in Jiaozhou Bay, China. *Front. Mar. Sci*. **9**, 900372. (doi:10.3389/fmars.2022.900372)
48. St. Pierre KA, Hunt BPV, Giesbrecht IJW, Tank SE, Lertzman KP, Del Bel Belluz J, Hessing-Lewis ML, Olson A, Froese T. 2022 Seasonally and spatially variable organic matter contributions from watershed, marine macrophyte, and pelagic sources to the Northeast Pacific coastal ocean margin. *Front. Mar. Sci*. **9**, 863209. (doi:10.3389/fmars.2022.863209)
49. Sukigara C, Otosaka S, Horimoto-Miyazaki N, Mino Y. 2023 Temporal variation of particulate organic carbon flux at the mouth of Tokyo Bay. *J. Oceanogr*. **79**, 199–209. (doi:10.1007/s10872-022-00660-7)
50. Nelson J, Hanson C, Koenig C, Chanton J. 2011 Influence of diet on stable carbon isotope composition in otoliths of juvenile red drum *Sciaenops ocellatus*. *Aquat. Biol*. **13**, 89–95. (doi:10.3354/ab00354)
51. Liu Q, Kandasamy S, Zhai W, Wang H, Veeran Y, Gao A, Chen CTA. 2022 Temperature is a better predictor of stable carbon isotopic compositions in marine particulates than dissolved CO_2 concentration. *Commun. Earth Environ*. **3**, 303. (doi:10.1038/s43247-022-00627-y)
52. Rau GH, Takahashi T, Des Marais DJ. 1989 Latitudinal variations in plankton $\delta^{13}C$: implications for CO_2 and productivity in past oceans. *Nature* **341**, 516–518. (doi:10.1038/341516a0)
53. Harris A, Mittaz J, Sapper J, Wick G, Zhu X, Dash P, Koner P. 2017 A new high-resolution sea surface temperature blended analysis. *Bull. Am. Meteorol. Soc*. **98**, 1015–1026. (doi:10.1175/BAMS-D-15-00002.1)

54. Lynch-Stieglitz J, Stocker TF, Broecker WS, Fairbanks RG. 1995 The influence of air-sea exchange on the isotopic composition of oceanic carbon: observations and modeling. *Glob. Biogeochem. Cycles* **9**, 653–665. (doi:10.1029/95gb02574)
55. Pancost RD, Freeman KH, Wakeham SG, Robertson CY. 1997 Controls on carbon isotope fractionation by diatoms in the Peru upwelling region. *Geochim. et Cosmochim. Acta* **61**, 4983–4991. (doi:10.1016/s0016-7037(97)00351-7)
56. Sexton JP, Montiel J, Shay JE, Stephens MR, Slatyer RA. 2017 Evolution of ecological niche breadth. *Annu. Rev. Ecol. Evol. Syst*. **48**, 183–206. (doi:10.1146/annurev-ecolsys-110316-023003)
57. Lin LH, Wiens JJ. 2016 Comparing macroecological patterns across continents: evolution of climatic niche breadth in varanid lizards. *Ecography* **40**, 960–970. (doi:10.1111/ecog.02343)
58. Dillon KS, Fleming CR, Slife C, Leaf RT. 2021 Stable isotopic niche variability and overlap across four fish guilds in the north-central Gulf of Mexico. Mar. Coast. Fish. **13**, 213–227. (doi:10.1002/mcf2.10148)
59. Kessler WS. 2006 The circulation of the eastern tropical Pacific: a review. Prog. Oceanogr. **69**, 181–217. (doi:10.1016/j.pocean.2006.03.009)
60. Rooker JR, Wells RJD, Artetxe-Arrate I, Arrizabalaga H, Fraile I, Dance MA *et al*. 2026 Supplementary material from: Otolith Geochemistry of Tropical and Temperate Tunas in the Ocean. Figshare. (doi:10.6084/m9.figshare.c.8285018)